Enhanced change detection performance based on deep despeckling of synthetic aperture radar images

IEEE Access
Multidisciplinary | Rapid Review | Open Access Journal

Date of publication xxxx 00, 0000, date of current version xxxx 00, 0000.

Digital Object Identifier 10.1109/ACCESS.2023.0322000

Enhanced Change Detection Performance Based on Deep Despeckling of Synthetic Aperture Radar Images

MOHAMED IHMEIDA[1], MUHAMMAD SHAHZAD[1]
[1]Department of Computer Science, University of Reading, Reading, RG6 6DH, UK (e-mail:m.a.g.ihmeida@pgr.reading.ac.uk, m.shahzad2@reading.ac.uk)
Corresponding author: Mohamed Ihmeida (e-mail: m.a.g.ihmeida@pgr.reading.ac.uk)

ABSTRACT

Synthetic aperture radar (SAR) image change detection (CD) focuses on identifying changes between two images at different times for the same geographical region. Recently, several deep learning methods have been proposed for performing SAR based CD. However, speckle noise remains a major challenge for these methods. To address this, we propose a despeckling model (DM) that effectively suppresses speckle noise and enhances the performance of the existing CD methods. The proposed despeckling architecture is not only resilient to multi-temporal SAR acquired from one SAR imaging process (i.e., the same number of SAR images looks before and after the change) but also deals with any combination of single or multi-look images acquired prior and after the change. Moreover, as a second contribution, we have also proposed a loss function that effectively suppresses speckle noise, thereby improving the change detection accuracy. Both the despeckling model and the proposed tolerant noise loss function are evaluated extensively on three public real SAR datasets, achieving superior performance compared to existing state-of-the-art SAR CD methods in all datasets.

INDEX TERMS Change Detection, Convolutional Neural Network, Despeckling Noise, Synthetic Aperture Radar, Unsupervised Learning.

I. INTRODUCTION

REMOTE sensing (RS) change detection (CD) aims to identify the change between two multi-temporal images for the same geographical region at different times [1] [2] [3] [4]. It offers valuable information for numerous applications, including deforestation monitoring [2], target detection [5], and agriculture investigation [6]. Moreover, the CD algorithms help to extract vital information to assess the change, especially in case of natural disasters (e.g., earthquakes, floods, droughts, and hurricanes [7] [8]), which in turn supports the local governments to make an effective and timely decision to prevent or mitigate material losses and lives.

In remote sensing, change detection endeavours to distinguish the changed and unchanged pixels of multi-temporal remote sensing images, this is Earth Observation (EO) images acquired for the same geographical region, but at different times [9] [10]. Typically, these multi-temporal images are co-registered (i.e., transformed into the same coordinate system) to obtain consistent radiometric characteristics such as brightness and contrast [11]. This enhances the change detection performance by aligning the correct position for each pixel in both multi-temporal images prior to feeding them as input to the subsequent change detection process [12] [13] [14] [15]. Most image registration algorithms rely on robust extraction of key points either using shallow extraction methods such as Scale-Invariant Feature Transform (SIFT) [16], Speeded-Up Robust Features (SURF) [17] or deep methods including convolutional neural networks (CNNs) [18], Siamese networks [19], and spatial transformer networks [20].

Once co-registered, the change map (a result of the change detection algorithm) can be easily obtained using classical change detection methods by computing a difference image (DI), simply the intensity difference between the two images. However, change detection in EO is nontrivial owing to inherent challenges such as errors in co-registration, variations in illumination, viewpoint, shadows, atmospheric effects (e.g., presence of clouds, fog, etc.), and varying sensor characteristics. Moreover, surface reflectance from incoherent objects (such as vegetation) can adversely affect the performance of optical CD algorithms.

Synthetic aperture radar (SAR) offers distinct advantages

over optical sensors for CD in EO because it is not affected by weather conditions, provides penetration through clouds and vegetation, and offers sensitivity to small changes, making it capable of detecting changes that may be missed by optical CD methods. This technique allows us to remotely map the reflectivity of objects or environments with high spatial resolution through the emission and reception of electromagnetic signals in the microwave spectrum, which enables ease of penetration through clouds and provides all-weather day/night sensing capability, making it suitable for applications related to disaster assessment (such as flooding and earthquake) [21].

Typically, optical CD methods rely mainly on supervised machine learning approaches [22] [23] [24]. However, owing to the lack of annotated SAR datasets, the majority of SAR CD approaches primarily rely on unsupervised learning [25] [26] [27]. Several methods for unsupervised SAR CD have been proposed in literature. For instance, Celik [28] proposed a simple unsupervised CD method using principal component analysis and k-means where change detection was achieved by partitioning the feature vector space into two clusters. Krinidis et al. [29] proposed fuzzy local information C-means (FLICM) to improve the clustering quality and aim to be robust to noise and preserve the image details. Gong et al. [30] also proposed fuzzy c-means (FCM), a reformulated FLICM to cluster image pixels into changed and unchanged. The aforementioned methods are performed under speckle-free images. These approaches perform fairly well. However, SAR data suffer from speckle noise, which arises owing to the coherent nature of SAR imaging, which causes interference patterns in the received signals. This speckle noise makes information extraction from SAR images challenging and, consequently, adversely affects change detection accuracy [31] [32] [33].

Several approaches have been proposed to address speckle noise. For instance, pioneering work in the despeckling of SAR images was proposed by Lee et al. [34]. Later, Lee [35] refined [36] to remove noisy edge boundaries in SAR images by enhancing the edge representation using local statistics (average and variance) within a 7x7 window. However, a drawback of this approach is its reliance on a fixed mask size [21]. Kuan et al. [37] proposed an adaptive speckle-noise smoothing filter that can handle different noise types without prior knowledge of the original statistics of the image. However, it tends to over smooth image details and has high computational complexity. Lope et al. [38] then proposed an Enhanced Lee filter and comprehensively analysed well-known filters by experimenting with varying the local coefficients of despeckled SAR images. Their approach allows the preservation of fine details, such as texture and edge information, in the heterogeneous regions of the observed SAR image. Zhu et al. [39] further improved despeckling performance by combining an enhanced Lee filter with a median filter.

In the context of change detection, several recent approaches have tackled the despeckling problem using deep neural networks. For instance, Zhang et al. [40] proposed unsupervised change detection using deep learning methods that employ multi-scale superpixel reconstruction method to suppress the speckle noise and generate a difference image. Subsequently, two-stage centre-constrained fuzzy c-means clustering algorithm is executed to classify the DI pixel into changed, unchanged and intermediate classes. Image patches belonging to changed and unchanged pixels are used as pseudo-label training samples, whereas the image patches belonging to the intermediate class are utilised as testing samples. The final stage is to train a convolutional wavelet neural network on the image patches belonging to changed and unchanged pixels to classify the intermediate classes. Wang et al. [41] introduced a sparse model that exploits structural features of changed regions in noisy DIs generated from multi-temporal SAR images. Wenhua et al. [42] introduced a multi-objective sparse feature learning mode. In this model, the sparsity of representation is dynamically learned to enhance robustness against various noise levels. The network is further fine-tuned using correctly labelled samples chosen from coarse results, allowing for learning semantic information related to changed and unchanged pixels. Liu et al. [43] presented a local restricted CNN for SAR change detection in which the original CNN was improved by incorporating a local spatial constraint. Qu et al. [44] also presented a dual domain neural network (DDNet) to obtain features from spatial and frequency domains to minimise the speckle noise. Gao et al. [3] proposed a Siamese adaptive fusion network for SAR image change detection to extract high-level semantic features from multi-temporal SAR images and suppress speckle noise. Meng et al. [45] proposed a robust loss function and a layer attention-based noise-tolerant network (LANTNet) that benefits from feature correlations among multi-convolutional layers and suppresses the impact of noisy labels.

Although these state-of-the-art deep learning-based approaches provide some robustness against different noise types, they still fail to fully suppress speckle noise, which hinders their effective change detection ability. Moreover, the amount of speckle noise varies between single-look or multi-look SAR imaging processes [6]. This is considered at different times (e.g., single-look at time instance t_1 and multi-look at time instance t_2) and consequently further degrades the performance of various change detection algorithms. To this end, in this paper, we propose a robust despeckling architecture that is not only resilient to multi-temporal SAR acquired from one SAR imaging process (i.e., the same number of SAR images looks before and after the change) but also deals with any combination of single or multi-look images acquired prior and after the change. To achieve this, the following are the significant contributions of this study:

- We propose a deep convolutional neural network-based Despeckling Model (DM) that can suppress speckle noise and improve the performance of state-of-the-art SAR CD methods.

- We develop a new speckle noise tolerant loss function, inspired by the works of [45], that is more resistant to speckle noise and significantly improves the baseline change detection accuracy.
- Both the despeckling model and the proposed tolerant noise loss function are evaluated on three public real SAR datasets and achieved superior performance compared with existing state-of-the-art SAR CD methods.

II. RELATED WORK

SAR change detection has been widely used in many applications such as urban extension [46], agricultural monitoring [47], target detection [48] disaster monitoring [49] and assessment [50]. Typically owing to the lack of annotated SAR datasets, most researchers rely on unsupervised methods [3] [51] [52] [53] to address SAR CD. However, the problem is highly challenging owing to the presence of speckle noise, which negatively impacts SAR images and reduces the change detection accuracy [31] [32] [54]. For this purpose, many researchers have formulated SAR CD in three sequential steps image pre-processing, difference image (DI) generation, and classification [55]. The image pre-processing stage includes despeckling (denoising) and image registration. Image despeckling aims to reduce the impact of speckle noise and enhance SAR image quality. However, oversmoothing usually occurs in doing so, which may result in the loss of geometric details. After despeckling, the latter image registration aids in aligning multi-temporal images in the same reference coordinate system, enabling accurate change detection [12] [13]. To generate difference image, various methods have been proposed in the literature, including image differencing (also known as subtracting) [2], log ratio [56], neighbourhood-based ratio [57], Gauss-ratio operator [58] and mean- and log-ratio difference [59]. Finally, the classification of DI typically includes thresholding and clustering [60].

Some approaches use the clustered DI image (preclassification result) to subsequently train a classifier model and then combine the information from the preclassification and classifier results to generate a change map. For instance, Gao et al. [61] computed the preclassification result by computing a DI via log-ratio and fuzzy c-means clustering and later trained the PCANet model (classifier) to obtain the initial classification, which was fused with the preclassification results to obtain the final change map. Similarly, Gao et al. [62] proposed an approach that employs a neighbourhood-based ratio to generate the difference image and then adopts an extreme learning machine (ELM) to model the high probability pixel based on the difference image, which is later used with the initial change map to yield the final change map. Wang et al. [63] employed a semi-supervised Laplacian support vector machine (SVM) to differentiate between changed and unchanged regions. To initialise the SVM, a pseudo-training set is generated using saliency similarity detection. This pseudo-training set consists of labelled changed and unchanged pixels. The Laplacian SVM effectively utilises the prior information from the available labelled samples and incorporates unlabelled samples to improve its discriminatory capabilities. Lv et al. [64] presented feature learning utilising a stacked contractive autoencoder to extract temporal change features from superpixels while effectively suppressing noise. Li et al. [65] proposed a Gamma correction and fuzzy local information c-means clustering model to reduce the impact of speckle noise and improve the performance. Liu et al. [43] introduced a locally restricted CNN for SAR change detection. They enhanced the original CNN architecture by incorporating a local spatial constraint, thereby improving CD performance.

Recently, a few approaches have aimed to explicitly suppress the inherent speckle noise to improve the SAR CD performance. For example, Qu et al. [44] proposed DDNet, a method that leverages features extracted from both the spatial and frequency domains to mitigate the impact of speckle noise. Gao et al. [3] also presented a Siamese adaptive fusion network for SAR image change detection, which focused on extracting high-level semantic features from multi-temporal SAR images while effectively suppressing speckle noise. Meng et al. [45] introduced a layer attention module that leverages the correlation among multiple convolutional layers and designed a loss function that minimises the influence of speckle noise, thereby enhancing the change detection performance. A limitation of these approaches is their inability to effectively tackle different speckle noises in images prior and after the change, for example, single-look prior image and multi-look post-change image, which makes it difficult for SAR CD methods to perform well due to varying speckle-noise characteristics [6]. In the following, we present a denoising framework that enables us to effectively tackle the SAR CD problem for both the same or different numbers of looks in the pre- and post-change images.

III. METHODOLOGY

The proposed methodology consists of two modules where the first despeckling modules where the first despeckling module passes the input SAR image through a series of convolutional layers to suppress speckle noise and later feeds the resulting noise-reduced image to the subsequent change detection module. For change detection, we adapt [45], which first performs a preclassification step and then employs a layer attention module that exploits the correlations among the multi-layer convolutions and produces robust cascaded feature representations learned by the network. Furthermore, we propose a noise-tolerant loss function that is resilient to speckle noise and significantly improves baseline change detection accuracy. In the following, we discuss them in detail, where we first present the proposed despeckling architecture, despeckling loss function, and adaptations that we have made to the baseline change detection approach by proposing a noise-resilient loss function.

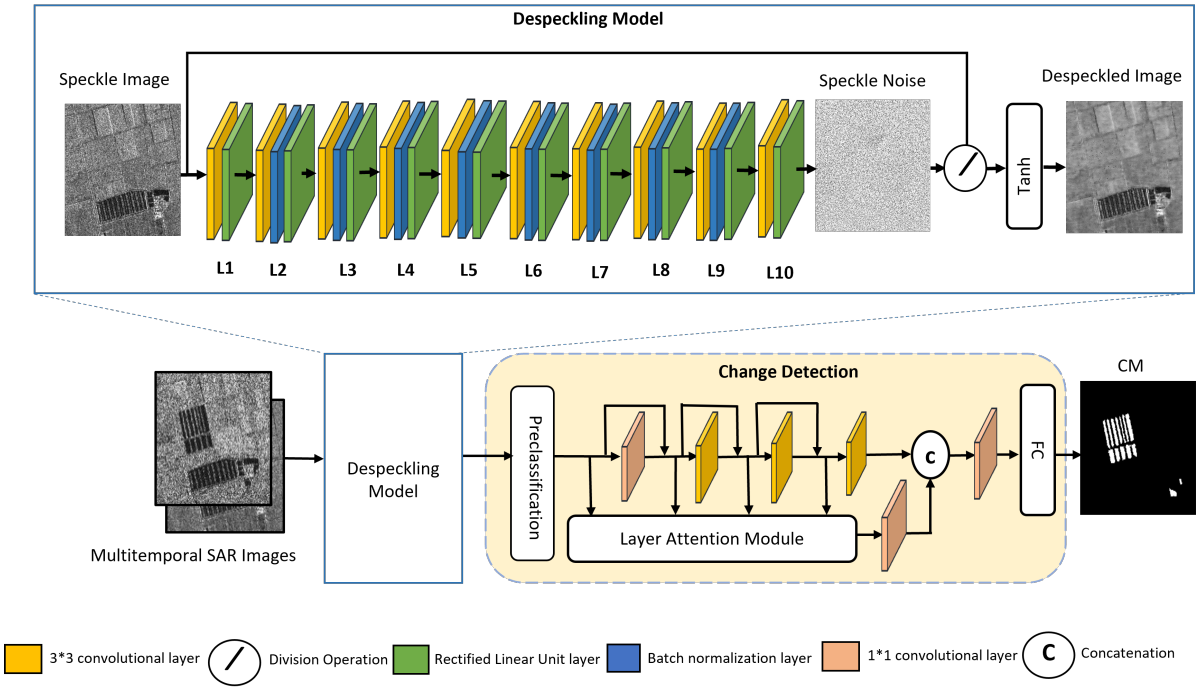

FIGURE 1: Proposed method for despeckling of SAR images for improved change detection task.

A. PROPOSED DESPECKLING ARCHITECTURE

The proposed despeckling architecture aims to learn a mapping from the input SAR image through a series of convolutional layers to yield a residual image [66] that contains speckle noise only. The learned residual (i.e., speckle-only in our case) image can then be passed along with the original image through either a subtraction [67] or division [68] operation to produce the resulting despeckled image. However, the division operation is preferable [68] because it avoids an additional logarithmic transformation step and enables end-to-end learning.

Practically, training such a network design requires ground truth or reference despeckled images, which is usually not the case for SAR images. To cope with this, several researchers synthetically generate reference noise-free SAR images using multiplicative noise models [69]. For our purpose, we also rely on synthetically generated SAR reference images and use them to train our proposed despeckling network architecture as depicted in Figure 1. It consists of ten convolutional layers, each incorporating batch normalisation and ReLU activation functions. Each layer has 64 filters with a stride of one, and zero padding is used to ensure that the output of each layer has the same dimensions as the input image, except for the last one, which has only one filter. At the end of the network, a hyperbolic tangent is employed as a nonlinear function [68]. For clarity, we also provide the architecture details of the proposed model along with the hyperparameter details in Table 1.

TABLE 1: Proposed Despeckling Model Configuration. where L1 and L10 refer to a series of Conv-ReLU layers, while the layers between L2 and L9 consist Conv-BN and ReLU layers as illustrated in Figure 1.

-	layer	Filter Size	Filters	Output size
L1	Conv + ReLU	3*3*1	64	256*256*64
L2-L9	Conv + BN + ReLU	3*3*64	64	256 *256* 64
L10	Conv + ReLU	3*3*64	1	256 *256*1

B. DESPECKLING LOSS FUNCTION

Let us assume that $F \in \mathbb{R}^{W\times H}$ denotes the observed SAR image intensity with speckle, $X \in \mathbb{R}^{W\times H}$ represent the noise-free SAR image, and $N \in \mathbb{R}^{W\times H}$ represents the multiplicative speckle noise. Then we can describe the relation between the observed and noise-free SAR images as

$$F = N \odot X \tag{1}$$

Where $\odot$ denotes the Hadamard product (i.e., the element-wise multiplication) between N and X. As mentioned earlier, X is synthetically generated by multiplicative noise using the procedure explained in [69] [70] [71].

One straightforward approach to train the despeckling network with learning parameters θ is to simply use the predicted despeckled image and noise-free SAR image to compute the per-pixel Euclidean loss function L_E as follows:

$$L_E(\theta) = \frac{1}{W \cdot H} \sum_{w=1}^{W} \sum_{h=1}^{H} \|X^{(w,h)} - \hat{X}^{(w,h)}\|^2 \tag{2}$$

Where X is the reference image, and $\hat{X}$ is the despeckled image. W and H represent the width and height of an image. Although this simple Euclidean loss L_E has been effective

in solving numerous image restoration problems such as super-resolution [72], semantic segmentation [73], change detection [74], and style transfer [75], it usually produces several artifacts (e.g., unwanted distortions such as irregular patterns, pixelation, blurring, or other visual abnormalities) in the resulting estimated image [76]. To address this problem, Wang et al. [68] integrated a supplementary total variation (TV) loss into L_E, which somewhat removes the artifacts but oversmoothes the images, causing loss of information and consequently degrading the performance of change detection [41]. To overcome these issues, we utilised a structural similarity index (SSIM), originally proposed for image quality assessment [77], as an auxiliary to L_E to achieve a better trade-off performance by removing artifacts while maintaining the necessary information, which improves the change detection performance.

$$SSIM(X,\hat{X}) = \frac{(2\mu_X\mu_{\hat{X}} + C_1)\cdot(2\sigma_{X\hat{X}} + C_2)}{(\mu_X^2 + \mu_{\hat{X}}^2 + C_1)\cdot(\sigma_X^2 + \sigma_{\hat{X}}^2 + C_2)} \tag{3}$$

Where X and $\hat{X}$ are the reference (noise-free) and despeckled images, respectively, μ_X and $\mu_{\hat{X}}$ are the mean values of X and $\hat{X}$respectively. Similarly, σ_X and $\sigma_{\hat{X}}$ are the standard deviations of X and $\hat{X}$ respectively. While $\sigma_{X\hat{X}}$ is the covariance between X and $\hat{X}$. Finally, C_1 and C_2 are constants set to be 0.01 and 0.03 respectively [77].

The total loss is thus calculated as follows:

$$L_T = L_E(\theta) + \lambda_{\text{SSIM}} \cdot SSIM \tag{4}$$

Where L_T is the total loss and λ_{SSIM} represents the weighting of the auxiliary SSIM in the loss.

C. PROPOSED CHANGE DETECTION LOSS FUNCTION

Existing unsupervised change detection methods utilise clustering algorithms such as hierarchical Fuzzy C-Means [78] and Fuzzy C-Means (FCM) [79] to generate pseudo-labels with a high probability for network training. While this method solves the need for label data, errors commonly affect network performance. In addition to this, the attention mechanism is utilised to emphasise the essential parts of the input while disregarding irrelevant information, but it often neglects the correlations among multiple convolution layers. To address this limitation, Meng et al. [45] proposed a layer attention module to weigh features from different layers based on the learned correlation matrix. This module effectively combines spatial information from low-level layers with semantic information from high-level layers, emphasising informative layers and suppressing redundant ones. The process involves matrix multiplication to assign adaptive weights to the input feature groups, followed by calculating the attention matrix using a softmax operation. The weighted feature matrix is then multiplied by the attention matrix, reshaped, and combined with the original input to produce the final output. The change map is generated through a series of convolution and fully connected layers. The trained network can classify all pixels from the multitemporal SAR images to obtain the final change map. We adapt the training strategy and propose a loss function that is more noise resistant to speckle noise. However, this loss function does not provide satisfactory performance. To this end, we designed a robust loss function that is more resistant to speckle noise. The loss function combines MSE and Kullback-Leibler Divergence (KL). The loss function is expressed as follows:

$$L_{\text{MSE}}(X,\hat{X}) = \|X - \hat{X}\|^2 \tag{5}$$

$$L_{\text{KL}}(X,\hat{X}) = \hat{X}\cdot(\log\hat{X} - X) \tag{6}$$

$$L_T = \alpha L_{MSE} + \beta L_{KL} \tag{7}$$

where α and β are two weighting hyperparameters.

In our empirical study, α and β were set to 0.9 and 0.1 to trade off noise robustness and convergence efficiency. The KL acts similarly to CE with the difference that CE penalises the network based on its predictions, whereas KL mainly evaluates the disparity between the probability distribution predicted by the network and the distribution of the reference ground truth. Therefore, we argue that combining MSE and KL can provide a better change detection performance and suppress speckle noise (see Section IV-C2). In the following section, we present the results of our proposed methodology along with the training details.

IV. EXPERIMENTAL RESULTS & EVALUATION

In this section, we first introduced the datasets and employed evaluation metrics. Subsequently, we investigated the effectiveness of the proposed despeckling model coupled with the CD loss function to improve the change detection accuracy. Finally, the results were presented and evaluated by comparing them with those of state-of-the-art methods.

A. DATASETS

Two types of datasets were used in this paper. The first is the Berkeley Segmentation Dataset 500, widely employed to generate synthetic SAR images. In addition, real SAR images (for the purpose of change detection purpose) were employed to assess the model's performance. Both datasets are described in detail In the following subsections:

1) Synthetic SAR Images

The Berkeley Segmentation Dataset 500 (BSD-500) was originally developed to evaluate the segmentation of natural edges, including object contours, object interior and background boundaries [80]. It included 500 natural images with carefully manually annotated boundaries and edges of natural objects collected from multiple users. This dataset has been widely used to generate synthetic SAR images for the purpose of despeckling [69] [70] [71]. Inspired by these studies, we have used it to train our despeckling model.

2) Real SAR Images

For the purpose of change detection, we employed three real SAR image datasets that are multi-temporal and have been co-registered and corrected geometrically.

- *Farmland and Yellow River Datasets:* The images for both datasets were captured by RADARSAT-2 in the region of the Yellow River Estuary in China on 18th June 2008 (pre-change) and 19th June 2009 (post-change). The pre-change images are single-look, whereas the post-change images have been acquired via a multi-looks (four) imaging process. The single-look pre-change image is significantly influenced by speckle noise compared to the four-look post-change image [3]. The disparity between the single and four looks in these two SAR datasets poses a significant challenge for change detection methods.
- *Ottawa Dataset:* The images for this dataset were also captured by RADARSAT-2 in May 1997 (pre-change) and August 1997 (post-change) in the areas affected by floods [44] [53] [81]. Because of the single imaging process, both the pre- and post-change images are less affected by noise in this dataset.

As mentioned above, synthetic SAR images were utilised to train the proposed DM, as depicted in Figure 1. While the real SAR images were despeckled for the purpose of change detection.

B. EVALUATION METRICS

Quantitative evaluation indices, including precision (P), recall (R), overall accuracy (OA) and F1 score (F1) [82] [83] [84] were used in this study to evaluate the change detection process. These metrics were computed as follows:

$$R = \frac{TP}{(TP + FN)} \tag{8}$$

$$P = \frac{TP}{(TP + FP)} \tag{9}$$

$$OA = \frac{(TP + TN)}{(TP + FP + FN + TN)} \tag{10}$$

$$F1 = \frac{(2 \cdot P \cdot R)}{(P + R)} \tag{11}$$

Here TP, FP, TN, and FN represent the true positives, false positives, true negatives, and false negatives, respectively.

A higher P value indicates a decrease in the occurrence of false alarms, while a greater R value indicates a reduced rate of incorrect detections. OA measures the proportion of accurately detected pixels in the image. However, relying solely on these three metrics can lead to overestimating the outcome when the number of altered pixels is only a small part of the entire image. The F1 score is used to address this, which considers the limitations of P and R, providing a more comprehensive evaluation of performance. It is important to note that larger F1 values indicate better overall performance [85].

C. ABLATION STUDY

In this section, we initially investigate the performance of the proposed DM on $F1$ score using three real SAR CD datasets that are discussed in Section IV-A2. We then feed the despeckled SAR images by the proposed DM to five change detection methods PCA-k-means (PCAK) [28], NR-ELM [62], DDNet [44], LANTNet [45] and the proposed CD method where the DDNet and LANTNet are the current state-of-the-art CD methods. Furthermore, we investigate the performance of the proposed CD loss function on $F1$ score by comparing it with different loss functions.

1) Performance Investigation of Despeckling Model

To validate the effectiveness of the despeckling model, we compared the results of change detection methods with and without the despeckling model using three real SAR datasets. Figure 2, 3 and 4 demonstrates that the proposed despeckling model considerably enhanced the F1 score for existing (including state-of-the-art) change detection methods. In all these experiments, we empirically set the λ_{SSIM} to be 5 in the loss objective (4) as a tradeoff between despeckling and change detection performance. It is evident that the performance of the CD methods improves once we passed them through the proposed despeckling model in three SAR datasets. However, in Figure 4, the NR-ELM algorithm with DM obtained a lower F1 because Ottawa dataset is less affected by the speckle noise. This is why we see a higher F1 score even with all other methods without DM. Secondly, Compared to other methods, the NR-ELM is more resistant to speckle noise because of the inherent despeckling process encoded within its architecture. Therefore, the decline in the F1 score when we include the DM module, is due to the fact that an additional despeckling process oversmooths the input image, which subsequently decreases the F1 score. These results will be explained in more detail in section IV-D.

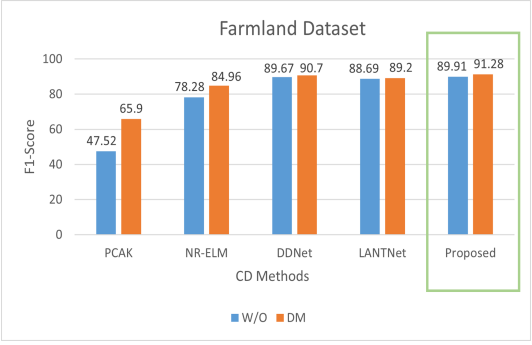

FIGURE 2: Relationship between DM and F1 score for Farmland dataset

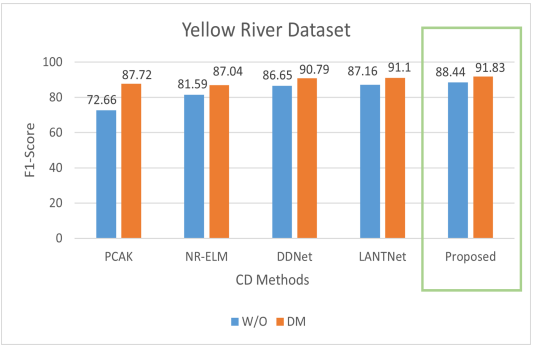

FIGURE 3: Relationship between DM and F1 score for Yellow River dataset

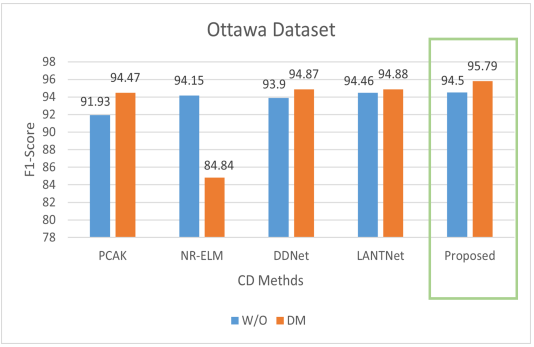

FIGURE 4: Relationship between DM and F1 score for Ottawa dataset

2) Performance Investigation of Proposed CD Loss Function

Furthermore, we compared various loss functions and analysed their performance over the baseline change detection methods. Table 2 shows that the loss function combining MSE and KL delivers the best performance, indicating its greater resilience to speckle noise.

TABLE 2: Relationship between loss functions and F1-Score.

Loss function	F1-Score		
	Farmland	Yellow River	Ottawa
MAE	89.1	87.24	94.24
MAE+CE [45]	88.69	87.16	94.46
MSE	86.91	86.22	94.75
MSE+CE(our)	89.60	88.23	94.54
MSE+KL(our)	**89.91**	**88.44**	**95.35**

D. EXPERIMENTAL RESULTS & DISCUSSION

To evaluate the impact of the proposed despeckling model on change detection purpose, we compare the effectiveness of the proposed DM with other existing despeckling methods such as Lee [34], Enhanced Lee [38], SAR2SAR [86] and IDCNN [68] on three real SAR datasets. Subsequently, we feed the despeckled SAR images to four aforementioned change detection methods, namely PCA-*k*-means (PCAK) [28], NR-ELM [62], DDNet [44] and LANTNet [45]. PCAK employs principle component analysis for feature extraction and utilises the *k*-means clustering algorithm for classification. NR-ELM incorporates the neighbourhood ratio for feature extraction using the difference image, followed by classification using an extreme learning machine. DDNet is a dual-domain network that exploits spatial and frequency domain features to mitigate speckle noise. LANTNet is a layer attention-based noise-tolerant network that leverages the correlation between convolutional layers. Both DDNet and LANTNet are currently state-of-the-art change detection methods.

Figures 5, 6 and 7 present the visual results of the change maps obtained from the aforementioned change detection methods using various despeckling filters on Farmland, Yellow River and Ottawa datasets respectively. The corresponding quantitative evaluations are provided in Tables 3, 4, and 5. In the tables, the w/o means it is the original method without despeckling. The DM is our proposed despeckling model, while the Proposed in Methods column refers to the baseline CD with the proposed objective loss function. Figures 5, 6 and 7 are organised as following; the first two columns represent Farmland dataset at time T1 and time T2, while column three represents the reference change detection images used as ground truth (GT). Columns four to eight display the results of PCAK, NR-ELM, DDNet, LANTNet and the proposed method, respectively. The row one presents the results of the above-mentioned methods without despeckling, while rows two to six represent the despeckling method results with Lee [34], Enhanced Lee [38], SAR2SAR [86], IDCNN [68] and DM (our) respectively. In the following section, we discuss the details of the achieved results for individual datasets.

1) Results of Farmland dataset

From Figure 5, it can be observed that the change map generated by PCAK misclassifies many unchanged pixels compared to GT. The Enhanced Lee filter significantly improves the results for PCAK, increasing the accuracy from 47.44% to 79.44%, while the proposed DM achieves 65.90%. It is worth mentioning that, Farmland dataset is heavily influenced by speckle noise, and change detection algorithms usually perform poorly compared to Ottawa dataset, which is less affected by speckle noise. Simply applying PCAK, which is a simple CD method, without despeckling, results in poor performance, as shown in Table 3. Another reason for this poor performance, in addition to the speckle noise, is because the pre- and post-change images in Farmland dataset are different looks, i.e., single and multi-looks before and after the change with varying noise levels. Using despeckling process somewhat takes this into account and improves the performance, as seen in Table 3, where all despeckling methods consistently improve the results with PCAK. Specifically, the Enhanced Lee performs the best here because it is well suited for stronger speckle noise and helps PCAK to significantly smooth the image, while DM is designed to support and generically enhance the overall CD performance. NR-ELM produces better results with less noise but misses some changed pixels. The DM filter improves NR-ELM's performance from 78.28% to 84.96%.

Furthermore, DDNet performed better than PCAK and

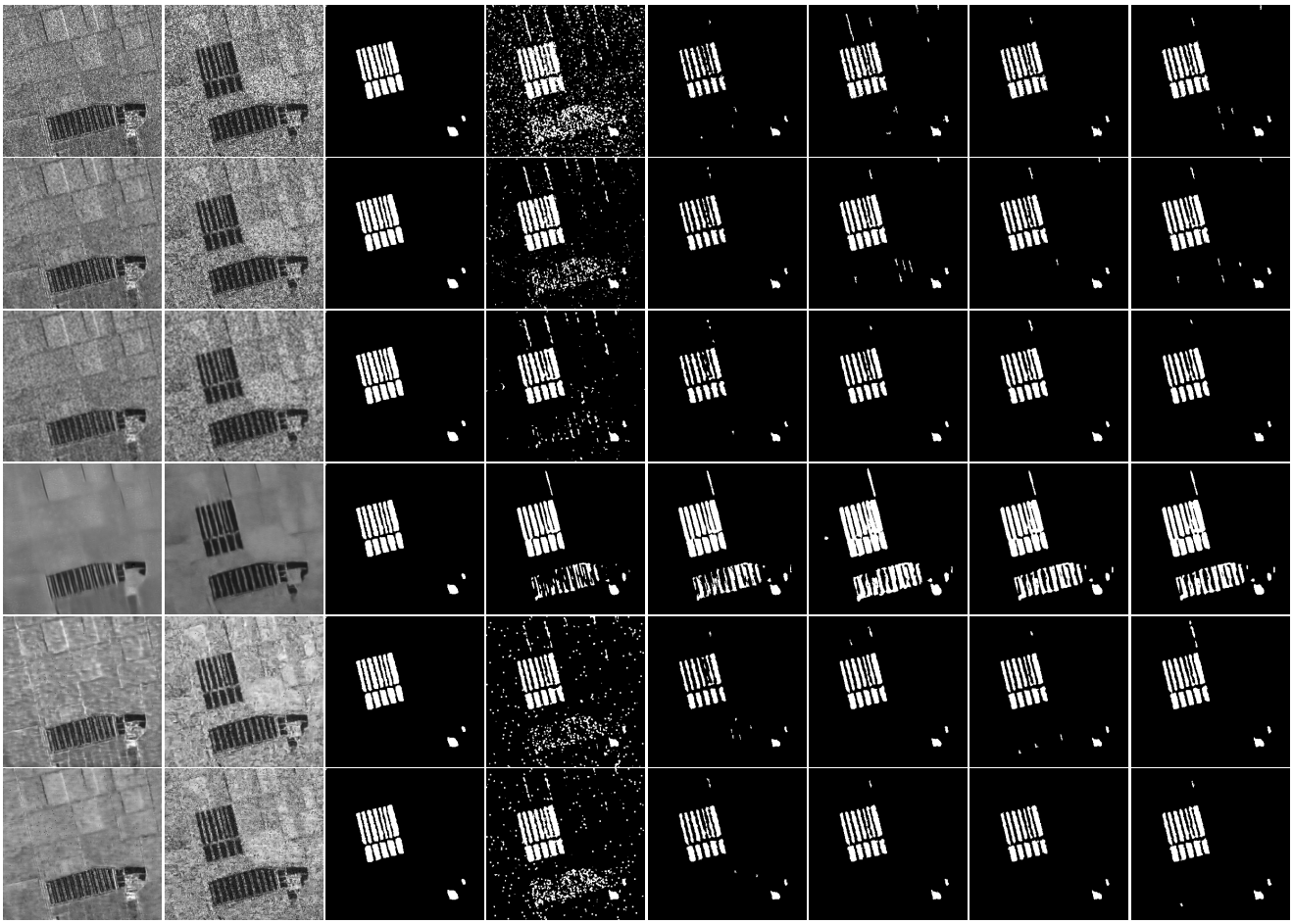

(a) Farm T1 (b) Farm T2 (c) GT (d) PCAK (e) NR-ELM (f) DDNet (g) LANTNet (h) Proposed

FIGURE 5: Visualised results of Farmland dataset with different despeckling methods. Rows: (1st row) Farmland without despeckling (w/o), (2nd row) Farmland despeckled with lee, (3rd row) Farmland despeckled with enhanced lee, (4th row) Farmland despeckled with SAR2SAR, (5th row) Farmland despeckled with IDCNN, (6th row) Farmland despeckled with proposed DM. Columns: Farmland image captured at (a) t1 and (b) t2. (c) refers to the ground truth (GT) image. Results obtained by methods (d) PCAK [28], (e) NR-ELM [62], (f) DDNet [44], (g) LANTNet [45], and (h) Proposed loss objective function.

NR-ELM did. The DM enhances the F1 score for DDNet from 86.67% to 89.70%, i.e., it demonstrates higher accuracy than PCAK and NR-ELM, although slightly lower than DDNet, while DM improves the accuracy of LANTNet from 88.69% to 89.20%. The proposed method improved performance after incorporating the DM module, increasing accuracy from 89.91% to 91.28%. Notably, the despeckled data using the SAR2SAR filter performed poorly and yielded lower results than the original methods without the despeckling model. It is evident that the DM outperforms other despeckling methods in terms of the F1 score for the purpose of change detection. Moreover, it consistently outperforms other change detection methods without a DM. It is primarily due to the fact that the proposed loss function is more resistant to speckle noise. In other words, the DM suppresses speckle noise even when two Farmland image pairs have different looks, such as single-look (pre-change) and four-look (post-change). This type of suppression is reflected positively in the performance of the change detection methods as shown in Table 3.

2) Results of the Yellow River dataset

In Figure 6, it is noticeable that the change map generated by PCAK misclassifies many unchanged pixels as changed ones compared with the GT. The Lee filter reduces speckle noise and improves the CM. The DM performs as the best filter, effectively suppressing noise and significantly improving the F1 score from 72.66% to 87.7% for the PCAK method. NR-ELM produces better results with less noise but misses some changed pixels, whereas the DM filter enhances NR-ELM's performance from 81.59% to 87.04%.

Furthermore, DDNet outperformed PCAK and NR-ELM results. The DM considerably enhance the F1 score from DDNet from 86.65% to 90.79%. LANTNet achieves higher accuracy than PCAK and NR-ELM. DM has enhanced the F1-score for LANTNet from 88.44% to 91.1%. After applying the proposed DM, the proposed method's performance has improved from 88.44% to 91.83%. Finally, the proposed method consistently outperforms all other change detection methods even without despeckling. With DM filtering, the

TABLE 3: Quantitative evaluation on Farmland change detection based on different despeckling filters.
Here w/o means it is the original method without despeckling, DM is our proposed despeckling model while the Proposed in Methods column refers to the baseline CD with the proposed objective loss function.

Methods	Metrics	w/o	Lee [34]	Enhanced Lee [38]	SAR2SAR [86]	ID-CNN [68]	DM
PCAK [28]	Recall↑	90.04	90.87	67.32	95.69	85.45	90.76
	Precision↑	32.27	57.73	96.89	66.51	54.35	51.74
	OA↑	88.22	95.53	97.94	96.89	94.89	94.44
	F1-Score↑	47.52	70.60	**79.44**	78.48	66.44	65.90
NR-ELM [62]	Recall↑	65.20	68.82	66.52	97.50	66.64	75.39
	Precision↑	97.92	99.13	98.51	57.17	97.23	97.33
	OA↑	97.86	98.12	97.96	95.52	97.91	98.42
	F1-Score↑	78.28	81.24	79.42	72.08	79.08	**84.96**
DDNet [44]	Recall↑	82.26	86.58	78.25	99.26	81.52	82.81
	Precision↑	91.59	92.76	98.21	48.66	97.57	97.85
	OA↑	98.50	98.81	98.63	93.76	98.79	98.87
	F1-Score↑	86.67	89.57	87.11	65.30	88.82	**89.70**
LANTNet [45]	Recall↑	81.35	80.51	81.76	98.46	79.87	81.18
	Precision↑	97.50	96.14	96.27	52.74	96.98	98.98
	OA↑	98.77	98.66	98.73	94.69	98.66	98.84
	F1-Score↑	88.69	87.64	88.42	68.69	87.60	**89.20**
Proposed	Recall↑	84.08	85.48	79.09	97.59	97.59	86.45
	Precision↑	97.50	93.78	97.22	53.08	53.08	96.67
	OA↑	98.89	98.81	98.63	94.75	94.75	99.02
	F1-Score↑	**89.91**	89.44	87.22	68.76	68.76	**91.28**

results even further improve.

It is worth mentioning that the despeckled data using the SAR2SAR filter does not perform well and yields lower results compared to the original methods without despeckling, such as DDNet and LANTNet. It is evident that DM achieves a superior F1 score for change detection methods compared to other despeckling methods due to the ability to efficiently cope with the single-look pre-change and multi-look post-change SAR images via robust loss function.

3) Results of the Ottawa dataset

Compared to previous datasets, the Ottawa dataset is less affected by speckle noise. This is evident from the achieved better change detection results of 91.93% using the PCAK method without any despeckling process on Ottawa dataset compared to the previous two datasets. Including the proposed DM further improves the F1 score value from 91.93% to 94.47%. NR-ELM provides better results compared to PCAK, Lee slightly improves the F1 score from 94.15% to 94.77%, whereas DM reduces the performance to 84.84% as shown in Figure 7 and Table 5. The proposed DM with the NR-ELM degrades the performance because of oversmoothing. This is because NR-ELM has an inherent despeckling process encoded within its architecture. Moreover, this is also the case for other despeckling methods except the Lee method, which does not degrade (but slightly improve) the performance. A possible reason for this could be because, in comparison, Lee [34] is the least strong despeckling method and therefore does not result in much oversmoothing, which degrades the performance.

DDNet performed better than PCAK and NR-ELM, and the proposed DM improves the F1 score for DDNet from 93.90% to 94.87%. LANTNet produces better accuracy than PCAK, NR-ELM and DDNet. Its accuracy has further improved by the proposed DM from 94.46% to 94.88%. With the proposed loss objective, the performance slightly improves from 94.46% to 94.50%, which is further enhanced from 94.50% to 95.79% when used in conjunction with the DM as shown in Figure 7 and Table 3. It can be observed from the Ottawa dataset results that the CD methods without despeckling already perform well because the data is less affected by noise. Nevertheless, with DM, the performance of these CD methods was further improved.

E. TRAINING SETUP

All the experiments were conducted on three data sets detailed in section IV-A where Python 3.7 with OpenCV version 3.4.2.17 was used. The hardware specifications include a Tesla GPU P100-PCIE-16 GB RAM 147.15 GB Disk.

V. CONCLUSION & OUTLOOK

In recent years, many deep-learning architectures have been employed for SAR change detection problems, leading to enhancements in the change detection performance. However, speckle noise remains a major challenge for these methods. To address this, we propose which are two-fold: 1) First, we have proposed a despeckling model which effectively suppresses the speckle noise and enhances the performance of existing CD methods; 2) Secondly, we have proposed a robust loss function that is able to take the performance of CD methods even further. The proposed solutions have been extensively examined and compared to the state-of-art SAR change detection methods. The achieved results with the proposed despeckling model and the noise tolerant loss function demonstrate superior performance compared to the current change detection methods. The proposed approach

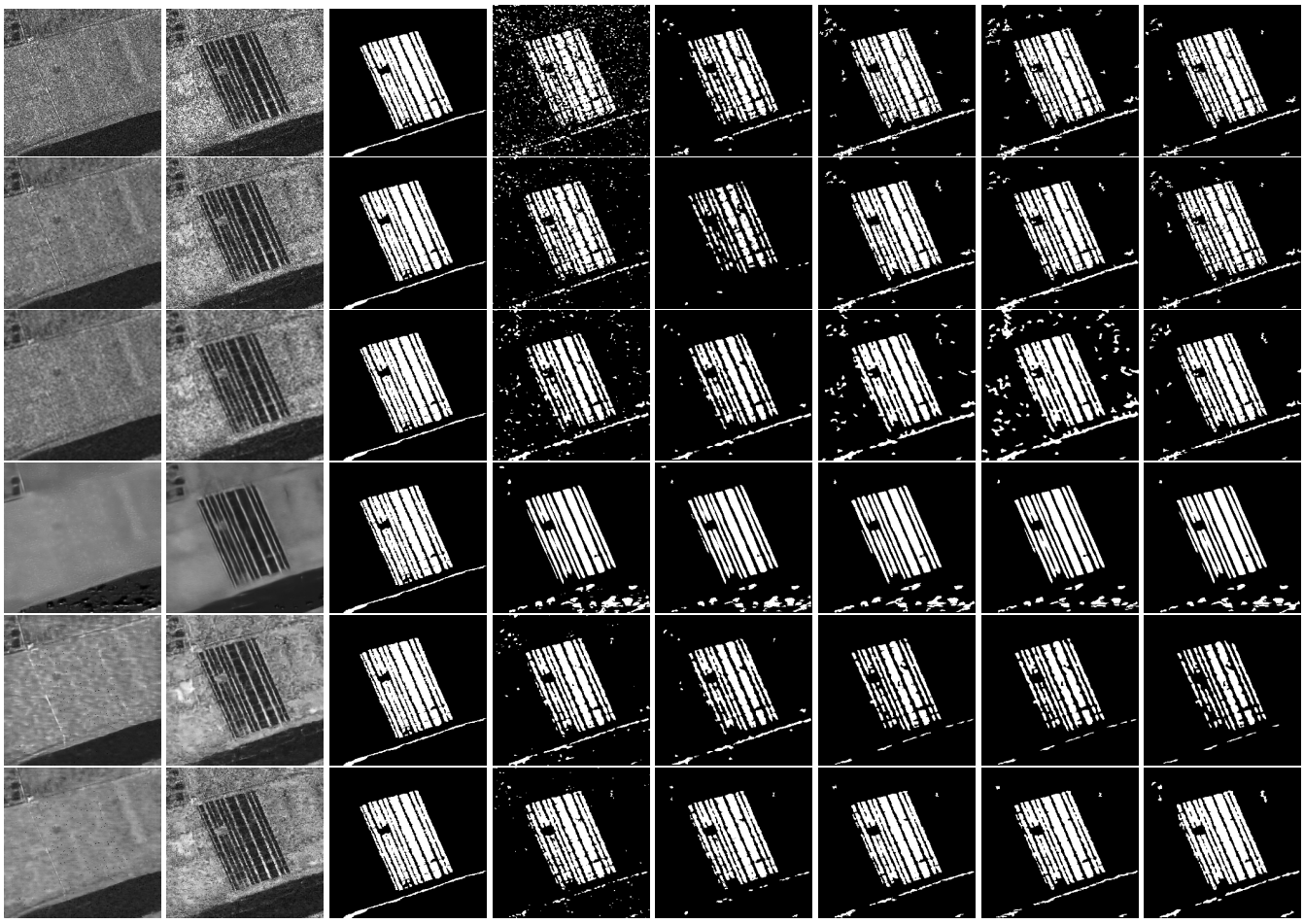

(a) Yellow T1 (b) Yellow T2 (c) GT (d) PCAK (e) NR-ELM (f) DDNet (g) LANTNet (h) Proposed

FIGURE 6: Visualised results of Yellow River dataset with different despeckling methods. Rows: (1st row) Farmland without despeckling (w/o), (2nd row) Farmland despeckled with lee, (3rd row) Farmland despeckled with enhanced lee, (4th row) Farmland despeckled with SAR2SAR, (5th row) Farmland despeckled with IDCNN, (6th row) Farmland despeckled with proposed DM. Columns: Farmland image captured at (a) t1 and (b) t2. (c) refers to the ground truth (GT) image. Results obtained by methods (d) PCAK [28], (e) NR-ELM [62], (f) DDNet [44], (g) LANTNet [45], and (h) Proposed loss objective function.

TABLE 4: Quantitative evaluation on Yellow River change detection based on different despeckling filters.

Methods	Metrics	w/o	Lee [34]	Enhanced Lee [38]	SAR2SAR [86]	ID-CNN [68]	DM
PCAK [28]	Recall↑	74.96	78.40	74.52	81.80	81.37	82.59
	Precision↑	70.50	87.80	82.75	83.31	92.79	93.53
	OA↑	89.80	94.12	92.58	93.74	95.49	95.82
	F1-Score↑	72.66	82.84	78.42	82.55	86.70	**87.72**
NR-ELM [62]	Recall↑	72.18	48.35	70.19	78.30	79.76	79.32
	Precision↑	93.83	99.72	92.22	85.53	95.08	96.42
	OA↑	94.11	90.63	93.54	93.68	95.59	95.73
	F1-Score↑	81.59	65.13	79.71	81.76	86.75	**87.04**
DDNet [44]	Recall↑	83.46	86.32	82.86	80.46	64.06	86.58
	Precision↑	90.09	91.41	81.89	85.00	90.40	95.44
	OA↑	95.35	96.06	93.59	93.90	93.43	96.83
	F1-Score↑	86.65	88.79	82.37	82.67	77.91	**90.79**
LANTNet [45]	Recall↑	82.44	84.00	83.03	79.84	65.93	87.51
	Precision↑	92.45	91.18	71.49	87.83	99.04	94.99
	OA↑	95.61	95.64	90.94	94.35	93.72	96.91
	F1-Score↑	87.16	87.44	76.83	83.64	79.16	**91.1**
Proposed	Recall↑	84.08	85.93	81.51	79.08	61.89	89.53
	Precision↑	93.28	87.05	82.01	86.44	97.75	94.25
	OA↑	96.03	95.14	93.42	93.97	92.85	97.12
	F1-Score↑	**88.44**	86.49	81.76	82.59	75.79	**91.83**

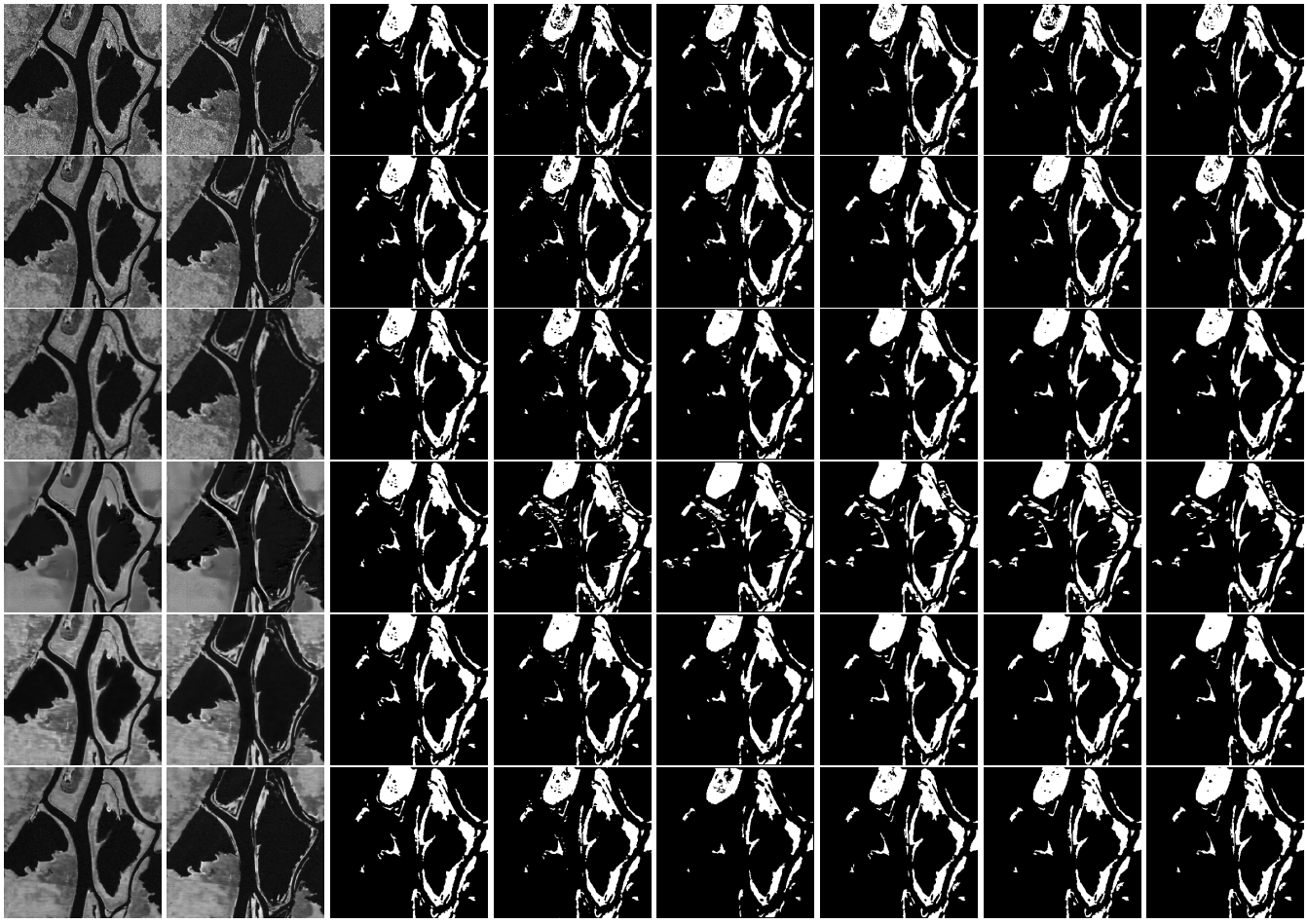

(a) Ottawa T1 (b) Ottawa T2 (c) GT (d) PCAK (e) NR-ELM (f) DDNet (g) LANTNet (h) Proposed

FIGURE 7: Visualised results of Ottawa dataset with different despeckling methods. Rows: (1st row) Farmland without despeckling (w/o), (2nd row) Farmland despeckled with lee, (3rd row) Farmland despeckled with enhanced lee, (4th row) Farmland despeckled with SAR2SAR, (5th row) Farmland despeckled with IDCNN, (6th row) Farmland despeckled with proposed DM. Columns: Farmland image captured at (a) t1 and (b) t2. (c) refers to the ground truth (GT) image. Results obtained by methods (d) PCAK [28], (e) NR-ELM [62], (f) DDNet [44], (g) LANTNet [45], and (h) Proposed loss objective function.

TABLE 5: Quantitative evaluation on Ottawa change detection based on different despeckling filters

Methods	Metrics	w/o	Lee [34]	Enhanced Lee [38]	SAR2SAR [86]	ID-CNN [68]	DM
PCAK [28]	Recall↑	88.16	91.58	88.74	88.85	92.01	91.00
	Precision↑	96.05	96.28	97.74	82.14	96.85	98.20
	OA↑	97.55	98.11	97.89	95.18	98.26	98.31
	F1-Score↑	91.93	93.87	93.02	85.36	94.37	**94.47**
NR-ELM [62]	Recall↑	93.14	94.79	87.67	88.68	92.07	73.92
	Precision↑	95.19	94.74	94.59	80.56	92.65	99.53
	OA↑	98.17	98.34	97.25	94.82	97.59	95.82
	F1-Score↑	94.15	**94.77**	91.00	84.42	92.36	84.84
DDNet [44]	Recall↑	92.70	93.66	93.66	90.78	94.51	91.71
	Precision↑	95.12	96.06	96.06	82.91	94.73	98.26
	OA↑	98.09	98.39	98.39	95.58	98.30	98.43
	F1-Score↑	93.90	94.84	94.85	86.67	94.62	**94.87**
LANTNet [45]	Recall↑	91.8	94.67	90.73	89.91	92.62	91.66
	Precision↑	97.30	94.48	95.11	82.49	95.23	98.33
	OA↑	98.3	98.28	97.80	95.39	98.1	98.44
	F1-Score↑	94.46	94.57	92.87	86.04	93.90	**94.88**
Proposed	Recall↑	91.70	92.74	88.80	91.88	93.11	93.73
	Precision↑	97.47	97.47	95.96	87.06	95.35	97.96
	OA↑	98.31	98.47	97.64	98.07	98.19	96.56
	F1-Score↑	**94.50**	95.04	92.24	89.41	94.22	**95.79**

so far only focuses on single-imaging modality. In future, an extension of the work could be in the domain of multi-modal (optical and SAR) change detection.

REFERENCES

[1] G. Quin, B. Pinel-Puyssegur, J.-M. Nicolas, and P. Loreaux, "Mimosa: An automatic change detection method for sar time series," *IEEE Transactions on Geoscience and Remote Sensing*, vol. 52, no. 9, pp. 5349–5363, 2013.

[2] L. Khelifi and M. Mignotte, "Deep learning for change detection in remote sensing images: Comprehensive review and meta-analysis," *IEEE Access*, vol. 8, pp. 126385–126400, 2020.

[3] Y. Gao, F. Gao, J. Dong, Q. Du, and H.-C. Li, "Synthetic aperture radar image change detection via siamese adaptive fusion network," *IEEE Journal of Selected Topics in Applied Earth Observations and Remote Sensing*, vol. 14, pp. 10748–10760, 2021.

[4] C. Chen, H. Ma, G. Yao, N. Lv, H. Yang, C. Li, and S. Wan, "Remote sensing image augmentation based on text description for waterside change detection," *Remote Sensing*, vol. 13, no. 10, p. 1894, 2021.

[5] X. Bai and F. Zhou, "Analysis of new top-hat transformation and the application for infrared dim small target detection," *Pattern Recognition*, vol. 43, no. 6, pp. 2145–2156, 2010.

[6] W. Shi, M. Zhang, R. Zhang, S. Chen, and Z. Zhan, "Change detection based on artificial intelligence: State-of-the-art and challenges," *Remote Sensing*, vol. 12, no. 10, p. 1688, 2020.

[7] Z. Zheng, Y. Zhong, J. Wang, A. Ma, and L. Zhang, "Building damage assessment for rapid disaster response with a deep object-based semantic change detection framework: From natural disasters to man-made disasters," *Remote Sensing of Environment*, vol. 265, p. 112636, 2021.

[8] D. Qin, X. Zhou, W. Zhou, G. Huang, Y. Ren, B. Horan, J. He, and N. Kito, "Msim: A change detection framework for damage assessment in natural disasters," *Expert Systems with Applications*, vol. 97, pp. 372–383, 2018.

[9] Q. Shi, M. Liu, S. Li, X. Liu, F. Wang, and L. Zhang, "A deeply supervised attention metric-based network and an open aerial image dataset for remote sensing change detection," *IEEE transactions on geoscience and remote sensing*, vol. 60, pp. 1–16, 2021.

[10] X. Zhang, S. Cheng, L. Wang, and H. Li, "Asymmetric cross-attention hierarchical network based on cnn and transformer for bitemporal remote sensing images change detection," *IEEE Transactions on Geoscience and Remote Sensing*, vol. 61, pp. 1–15, 2023.

[11] H. Noh, J. Ju, M. Seo, J. Park, and D.-G. Choi, "Unsupervised change detection based on image reconstruction loss," in *Proceedings of the IEEE/CVF Conference on Computer Vision and Pattern Recognition*, pp. 1352–1361, 2022.

[12] M. Ihmeida and H. Wei, "Image registration techniques and applications: comparative study on remote sensing imagery," in *2021 14th International Conference on Developments in eSystems Engineering (DeSE)*, pp. 142–148, IEEE, 2021.

[13] L. Ma, Y. Liu, X. Zhang, Y. Ye, G. Yin, and B. A. Johnson, "Deep learning in remote sensing applications: A meta-analysis and review," *ISPRS journal of photogrammetry and remote sensing*, vol. 152, pp. 166–177, 2019.

[14] J. Zhang, W. Ma, Y. Wu, and L. Jiao, "Multimodal remote sensing image registration based on image transfer and local features," *IEEE Geoscience and Remote Sensing Letters*, vol. 16, no. 8, pp. 1210–1214, 2019.

[15] X. Dai and S. Khorram, "The effects of image misregistration on the accuracy of remotely sensed change detection," *IEEE Transactions on Geoscience and Remote sensing*, vol. 36, no. 5, pp. 1566–1577, 1998.

[16] D. G. Lowe, "Distinctive image features from scale-invariant keypoints," *International journal of computer vision*, vol. 60, no. 2, pp. 91–110, 2004.

[17] H. Bay, T. Tuytelaars, and L. Van Gool, "Surf: Speeded up robust features," in *European conference on computer vision*, pp. 404–417, Springer, 2006.

[18] H. Zhang, W. Ni, W. Yan, D. Xiang, J. Wu, X. Yang, and H. Bian, "Registration of multimodal remote sensing image based on deep fully convolutional neural network," *IEEE Journal of Selected Topics in Applied Earth Observations and Remote Sensing*, vol. 12, no. 8, pp. 3028–3042, 2019.

[19] R. Fan, B. Hou, J. Liu, J. Yang, and Z. Hong, "Registration of multiresolution remote sensing images based on l2-siamese model," *IEEE Journal of Selected Topics in Applied Earth Observations and Remote Sensing*, vol. 14, pp. 237–248, 2020.

[20] L. Li, L. Han, M. Ding, and H. Cao, "Multimodal image fusion framework for end-to-end remote sensing image registration," *IEEE Transactions on Geoscience and Remote Sensing*, vol. 61, pp. 1–14, 2023.

[21] P. Singh, M. Diwakar, A. Shankar, R. Shree, and M. Kumar, "A review on sar image and its despeckling," *Archives of Computational Methods in Engineering*, vol. 28, pp. 4633–4653, 2021.

[22] L. Xu, W. Jing, H. Song, and G. Chen, "High-resolution remote sensing image change detection combined with pixel-level and object-level," *IEEE Access*, vol. 7, pp. 78909–78918, 2019.

[23] G. M. Gandhi, B. Parthiban, N. Thummalu, and A. Christy, "Ndvi: Vegetation change detection using remote sensing and gis–a case study of vellore district," *Procedia computer science*, vol. 57, pp. 1199–1210, 2015.

[24] H. Chen and Z. Shi, "A spatial-temporal attention-based method and a new dataset for remote sensing image change detection," *Remote Sensing*, vol. 12, no. 10, p. 1662, 2020.

[25] F. Gao, X. Wang, Y. Gao, J. Dong, and S. Wang, "Sea ice change detection in sar images based on convolutional-wavelet neural networks," *IEEE Geoscience and Remote Sensing Letters*, vol. 16, no. 8, pp. 1240–1244, 2019.

[26] Y. Bazi, L. Bruzzone, and F. Melgani, "An unsupervised approach based on the generalized gaussian model to automatic change detection in multitemporal sar images," *IEEE Transactions on Geoscience and Remote Sensing*, vol. 43, no. 4, pp. 874–887, 2005.

[27] H.-C. Li, T. Celik, N. Longbotham, and W. J. Emery, "Gabor feature based unsupervised change detection of multitemporal sar images based on two-level clustering," *IEEE Geoscience and Remote Sensing Letters*, vol. 12, no. 12, pp. 2458–2462, 2015.

[28] T. Celik, "Unsupervised change detection in satellite images using principal component analysis and k-means clustering," *IEEE geoscience and remote sensing letters*, vol. 6, no. 4, pp. 772–776, 2009.

[29] S. Krinidis and V. Chatzis, "A robust fuzzy local information c-means clustering algorithm," *IEEE transactions on image processing*, vol. 19, no. 5, pp. 1328–1337, 2010.

[30] M. Gong, Z. Zhou, and J. Ma, "Change detection in synthetic aperture radar images based on image fusion and fuzzy clustering," *IEEE Transactions on Image Processing*, vol. 21, no. 4, pp. 2141–2151, 2012.

[31] H. Dong, W. Ma, Y. Wu, M. Gong, and L. Jiao, "Local descriptor learning for change detection in synthetic aperture radar images via convolutional neural networks," *IEEE Access*, vol. 7, pp. 15389–15403, 2019.

[32] N. Lv, C. Chen, T. Qiu, and A. K. Sangaiah, "Deep learning and superpixel feature extraction based on contractive autoencoder for change detection in sar images," *IEEE Transactions on Industrial Informatics*, vol. 14, no. 12, pp. 5530–5538, 2018.

[33] S. Saha, M. Shahzad, P. Ebel, and X. X. Zhu, "Supervised change detection using prechange optical-sar and postchange sar data," *IEEE Journal of Selected Topics in Applied Earth Observations and Remote Sensing*, vol. 15, pp. 8170–8178, 2022.

[34] J.-S. Lee, "Digital image enhancement and noise filtering by use of local statistics," *IEEE transactions on pattern analysis and machine intelligence*, no. 2, pp. 165–168, 1980.

[35] J.-S. Lee, "Speckle analysis and smoothing of synthetic aperture radar images," *Computer graphics and image processing*, vol. 17, no. 1, pp. 24–32, 1981.

[36] J.-S. Lee, "Refined filtering of image noise using local statistics," *Computer graphics and image processing*, vol. 15, no. 4, pp. 380–389, 1981.

[37] D. T. Kuan, A. A. Sawchuk, T. C. Strand, and P. Chavel, "Adaptive noise smoothing filter for images with signal-dependent noise," *IEEE transactions on pattern analysis and machine intelligence*, no. 2, pp. 165–177, 1985.

[38] A. Lopes, R. Touzi, and E. Nezry, "Adaptive speckle filters and scene heterogeneity," *IEEE Transactions on Geoscience and Remote Sensing*, vol. 28, no. 6, pp. 992–1000, 1990.

[39] J. Zhu, J. Wen, and Y. Zhang, "A new algorithm for sar image despeckling using an enhanced lee filter and median filter," in *2013 6th International congress on image and signal processing (CISP)*, vol. 1, pp. 224–228, IEEE, 2013.

[40] X. Zhang, H. Su, C. Zhang, X. Gu, X. Tan, and P. M. Atkinson, "Robust unsupervised small area change detection from sar imagery using deep learning," *ISPRS Journal of Photogrammetry and Remote Sensing*, vol. 173, pp. 79–94, 2021.

[41] R. Wang, J.-W. Chen, L. Jiao, and M. Wang, "How can despeckling and structural features benefit to change detection on bitemporal sar images?," *Remote Sensing*, vol. 11, no. 4, p. 421, 2019.

[42] W. Zhang, L. Jiao, F. Liu, S. Yang, W. Song, and J. Liu, "Sparse feature clustering network for unsupervised sar image change detection," *IEEE Transactions on Geoscience and Remote Sensing*, vol. 60, pp. 1–13, 2022.

[43] F. Liu, L. Jiao, X. Tang, S. Yang, W. Ma, and B. Hou, "Local restricted convolutional neural network for change detection in polarimetric sar images," *IEEE Transactions on Neural Networks and Learning Systems*, vol. 30, no. 3, pp. 818–833, 2019.

[44] X. Qu, F. Gao, J. Dong, Q. Du, and H.-C. Li, "Change detection in synthetic aperture radar images using a dual-domain network," *IEEE Geoscience and Remote Sensing Letters*, vol. 19, pp. 1–5, 2021.

[45] D. Meng, F. Gao, J. Dong, Q. Du, and H.-C. Li, "Synthetic aperture radar image change detection via layer attention-based noise-tolerant network," *IEEE Geoscience and Remote Sensing Letters*, vol. 19, pp. 1–5, 2022.

[46] Q. Shi, M. Liu, S. Li, X. Liu, F. Wang, and L. Zhang, "A deeply supervised attention metric-based network and an open aerial image dataset for remote sensing change detection," *IEEE Transactions on Geoscience and Remote Sensing*, vol. 60, pp. 1–16, 2022.

[47] R. E. Kennedy, P. A. Townsend, J. E. Gross, W. B. Cohen, P. Bolstad, Y. Wang, and P. Adams, "Remote sensing change detection tools for natural resource managers: Understanding concepts and tradeoffs in the design of landscape monitoring projects," *Remote sensing of environment*, vol. 113, no. 7, pp. 1382–1396, 2009.

[48] F. Hao, Z.-F. Ma, H.-P. Tian, H. Wang, and D. Wu, "Semi-supervised label propagation for multi-source remote sensing image change detection," *Computers & Geosciences*, vol. 170, p. 105249, 2023.

[49] E. Hamidi, B. G. Peter, D. F. Muñoz, H. Moftakhari, and H. Moradkhani, "Fast flood extent monitoring with sar change detection using google earth engine," *IEEE Transactions on Geoscience and Remote Sensing*, vol. 61, pp. 1–19, 2023.

[50] F. Wang and Y. J. Xu, "Comparison of remote sensing change detection techniques for assessing hurricane damage to forests," *Environmental monitoring and assessment*, vol. 162, pp. 311–326, 2010.

[51] Y. Li, C. Peng, Y. Chen, L. Jiao, L. Zhou, and R. Shang, "A deep learning method for change detection in synthetic aperture radar images," *IEEE Transactions on Geoscience and Remote Sensing*, vol. 57, no. 8, pp. 5751–5763, 2019.

[52] D. Xue, T. Lei, X. Jia, X. Wang, T. Chen, and A. K. Nandi, "Unsupervised change detection using multiscale and multiresolution gaussian-mixture-model guided by saliency enhancement," *IEEE Journal of Selected Topics in Applied Earth Observations and Remote Sensing*, vol. 14, pp. 1796–1809, 2020.

[53] J. Wang, F. Gao, J. Dong, S. Zhang, and Q. Du, "Change detection from synthetic aperture radar images via graph-based knowledge supplement network," *arXiv preprint arXiv:2201.08954*, 2022.

[54] Y. Li, C. Peng, Y. Chen, L. Jiao, L. Zhou, and R. Shang, "A deep learning method for change detection in synthetic aperture radar images," *IEEE Transactions on Geoscience and Remote Sensing*, vol. 57, no. 8, pp. 5751–5763, 2019.

[55] L. Bruzzone and D. F. Prieto, "An adaptive semiparametric and context-based approach to unsupervised change detection in multitemporal remote-sensing images," *IEEE Transactions on image processing*, vol. 11, no. 4, pp. 452–466, 2002.

[56] R. Dekker, "Speckle filtering in satellite sar change detection imagery," *International Journal of Remote Sensing*, vol. 19, no. 6, pp. 1133–1146, 1998.

[57] M. Majidi, S. Ahmadi, and R. Shah-Hosseini, "A saliency-guided neighbourhood ratio model for automatic change detection of sar images," *International Journal of Remote Sensing*, vol. 41, no. 24, pp. 9606–9627, 2020.

[58] B. Hou, Q. Wei, Y. Zheng, and S. Wang, "Unsupervised change detection in sar image based on gauss-log ratio image fusion and compressed projection," *IEEE journal of selected topics in applied earth observations and remote sensing*, vol. 7, no. 8, pp. 3297–3317, 2014.

[59] W. Zhang, L. Jiao, F. Liu, S. Yang, and J. Liu, "Adaptive contourlet fusion clustering for sar image change detection," *IEEE Transactions on Image Processing*, vol. 31, pp. 2295–2308, 2022.

[60] Y. Gao, F. Gao, J. Dong, Q. Du, and H.-C. Li, "Synthetic aperture radar image change detection via siamese adaptive fusion network," *IEEE Journal of Selected Topics in Applied Earth Observations and Remote Sensing*, vol. 14, pp. 10748–10760, 2021.

[61] F. Gao, J. Dong, B. Li, and Q. Xu, "Automatic change detection in synthetic aperture radar images based on pcanet," *IEEE Geoscience and Remote Sensing Letters*, vol. 13, no. 12, pp. 1792–1796, 2016.

[62] F. Gao, J. Dong, B. Li, Q. Xu, and C. Xie, "Change detection from synthetic aperture radar images based on neighborhood-based ratio and extreme learning machine," *Journal of Applied Remote Sensing*, vol. 10, no. 4, p. 046019, 2016.

[63] S. Wang, S. Yang, and L. Jiao, "Saliency-guided change detection for sar imagery using a semi-supervised laplacian svm," *Remote sensing letters*, vol. 7, no. 11, pp. 1043–1052, 2016.

[64] N. Lv, C. Chen, T. Qiu, and A. K. Sangaiah, "Deep learning and superpixel feature extraction based on contractive autoencoder for change detection in sar images," *IEEE transactions on industrial informatics*, vol. 14, no. 12, pp. 5530–5538, 2018.

[65] L. Li, H. Ma, and Z. Jia, "Gamma correction-based automatic unsupervised change detection in sar images via flicm model," *Journal of the Indian Society of Remote Sensing*, pp. 1–12, 2023.

[66] K. Zhang, W. Zuo, Y. Chen, D. Meng, and L. Zhang, "Beyond a gaussian denoiser: Residual learning of deep cnn for image denoising," *IEEE transactions on image processing*, vol. 26, no. 7, pp. 3142–3155, 2017.

[67] G. Chierchia, D. Cozzolino, G. Poggi, and L. Verdoliva, "Sar image despeckling through convolutional neural networks," in *2017 IEEE International Geoscience and Remote Sensing Symposium (IGARSS)*, pp. 5438–5441, IEEE, 2017.

[68] P. Wang, H. Zhang, and V. M. Patel, "Sar image despeckling using a convolutional neural network," *IEEE Signal Processing Letters*, vol. 24, no. 12, pp. 1763–1767, 2017.

[69] F. Ulaby, M. C. Dobson, and J. L. Álvarez-Pérez, *Handbook of radar scattering statistics for terrain*. Artech House, 2019.

[70] H.-C. Li, W. Hong, Y.-R. Wu, and P.-Z. Fan, "Bayesian wavelet shrinkage with heterogeneity-adaptive threshold for sar image despeckling based on generalized gamma distribution," *IEEE Transactions on Geoscience and Remote Sensing*, vol. 51, no. 4, pp. 2388–2402, 2012.

[71] S. Intajag and S. Chitwong, "Speckle noise estimation with generalized gamma distribution," in *2006 SICE-ICASE International Joint Conference*, pp. 1164–1167, IEEE, 2006.

[72] C. Dong, C. C. Loy, K. He, and X. Tang, "Learning a deep convolutional network for image super-resolution," in *Computer Vision–ECCV 2014: 13th European Conference, Zurich, Switzerland, September 6-12, 2014, Proceedings, Part IV 13*, pp. 184–199, Springer, 2014.

[73] J. Long, E. Shelhamer, and T. Darrell, "Fully convolutional networks for semantic segmentation," in *Proceedings of the IEEE conference on computer vision and pattern recognition*, pp. 3431–3440, 2015.

[74] Y. Liu, C. Pang, Z. Zhan, X. Zhang, and X. Yang, "Building change detection for remote sensing images using a dual-task constrained deep siamese convolutional network model," *IEEE Geoscience and Remote Sensing Letters*, vol. 18, no. 5, pp. 811–815, 2021.

[75] L. A. Gatys, A. S. Ecker, and M. Bethge, "Image style transfer using convolutional neural networks," in *Proceedings of the IEEE conference on computer vision and pattern recognition*, pp. 2414–2423, 2016.

[76] M. Derezinski and M. K. K. Warmuth, "The limits of squared euclidean distance regularization," in *Advances in Neural Information Processing Systems* (Z. Ghahramani, M. Welling, C. Cortes, N. Lawrence, and K. Weinberger, eds.), vol. 27, Curran Associates, Inc., 2014.

[77] Z. Wang, A. C. Bovik, H. R. Sheikh, and E. P. Simoncelli, "Image quality assessment: from error visibility to structural similarity," *IEEE transactions on image processing*, vol. 13, no. 4, pp. 600–612, 2004.

[78] Y. Zheng, B. Jeon, D. Xu, Q. Wu, and H. Zhang, "Image segmentation by generalized hierarchical fuzzy c-means algorithm," *Journal of Intelligent & Fuzzy Systems*, vol. 28, no. 2, pp. 961–973, 2015.

[79] J. C. Bezdek, R. Ehrlich, and W. Full, "Fcm: The fuzzy c-means clustering algorithm," *Computers & geosciences*, vol. 10, no. 2-3, pp. 191–203, 1984.

[80] P. Arbelaez, M. Maire, C. Fowlkes, and J. Malik, "Contour detection and hierarchical image segmentation," *IEEE transactions on pattern analysis and machine intelligence*, vol. 33, no. 5, pp. 898–916, 2010.

[81] Y. Gao, F. Gao, J. Dong, and H.-C. Li, "Sar image change detection based on multiscale capsule network," *IEEE Geoscience and Remote Sensing Letters*, vol. 18, no. 3, pp. 484–488, 2020.

[82] A. Varghese, J. Gubbi, A. Ramaswamy, and P. Balamuralidhar, "Changenet: A deep learning architecture for visual change detection," in *Proceedings of the European conference on computer vision (ECCV) workshops*, pp. 0–0, 2018.

[83] X. Tang, H. Zhang, L. Mou, F. Liu, X. Zhang, X. X. Zhu, and L. Jiao, "An unsupervised remote sensing change detection method based on multiscale graph convolutional network and metric learning," *IEEE Transactions on Geoscience and Remote Sensing*, 2021.

[84] G. M. Foody, "Explaining the unsuitability of the kappa coefficient in the assessment and comparison of the accuracy of thematic maps obtained by image classification," *Remote Sensing of Environment*, vol. 239, p. 111630, 2020.
[85] Y. Chen and L. Bruzzone, "Self-supervised change detection in multi-view remote sensing images. arxiv 2021," *arXiv preprint arXiv:2103.05969*.
[86] E. Dalsasso, L. Denis, and F. Tupin, "Sar2sar: A semi-supervised despeckling algorithm for sar images," *IEEE Journal of Selected Topics in Applied Earth Observations and Remote Sensing*, vol. 14, pp. 4321–4329, 2021.

MOHAMED IHMEIDA received the BS.c degree in electrical and electronic engineering from University of Benghazi, Libya, in 2010, the MS.c degree in Advanced Computer Network from University of Derby, UK, in 2018. In 2019 started his PhD journey at University of Reading in Synthetic Radar Images change detection.

PLACE PHOTO HERE

MUHAMMAD SHAHZAD is currently working as a Lecturer in the Department of Computer Science, University of Reading, Reading, United Kingdom. His research interests include deep learning for remote sensing and computer vision-related applications.